JCTC Journal of Chemical Theory and Computation

Article

pubs.acs.org/JCTC

Non-covalent Interactions of CO_2 with Functional Groups of Metal–Organic Frameworks from a CCSD(T) Scheme Applicable to Large Systems

Konstantinos D. Vogiatzis,[†,‡] Wim Klopper,[‡] and Joachim Friedrich*[,§]

[†]Department of Chemistry, University of Minnesota, 207 Pleasant Street Southeast, Minneapolis, Minnesota 55455-0431, United States

[‡]Institute of Physical Chemistry, Karlsruhe Institute of Technology, Fritz-Haber-Weg 2, D-76131 Karlsruhe, Germany

[§]Institute of Chemistry, Chemnitz University of Technology, Strasse der Nationen 62, D-09111 Chemnitz, Germany

Supporting Information

ABSTRACT: The strength of interactions between CO_2 and 23 building blocks of metal–organic frameworks are reported in this paper. This theoretical study is based on an incremental, explicitly correlated coupled-cluster scheme with interference effects. This scheme allows the accurate calculation of molecular complexes such as zinc acetate (32 non-hydrogen atoms) at the CCSD(T) level, close to the basis set limit. Higher CO_2 affinity for complexes with nitrogen-containing heterocycles is predicted from the calculated interaction energies. The good agreement between the interaction energies obtained from the CCSD(T) scheme and DFT-D3 is discussed.

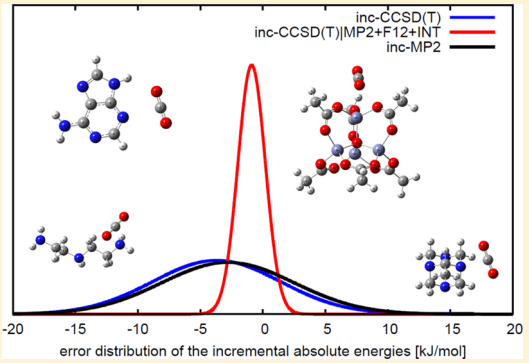

1. INTRODUCTION

Metal–organic frameworks (MOFs) offer high capacity and cyclability properties for CO_2 storage.[1−4] Different strategies have been used for enhancing CO_2 selectivity over other gases such as CH_4, H_2O, N_2, and alkenes. Such strategies include building blocks with open metal sites[5−7] or incorporation of functional polar groups, like amino groups[8−13] and nitrogen-containing heteroaromatics.[14−19] These CO_2-phile groups form stronger non-covalent interactions with CO_2 than CH_4 or N_2 and raise the separation efficiency of the MOFs while increasing the adsorption capacity of the material. The cause of stabilization between the CO_2-phile and CO_2 is a typical Lewis acid–Lewis base interaction. The strength of the interaction can be further increased by synergistic hydrogen bonds that involve one of the oxygens of CO_2.[18,20−23]

Theoretical simulations have been used to characterize MOFs for adsorption and have helped to elucidate mechanisms of CO_2 capture.[24−26] A multiscale theoretical investigation usually begins with electronic structure theory calculations on the interaction potentials between CO_2 and small models of the inorganic units, the organic linkers, or both. These potentials provide parameters for the development of accurate force fields which can describe CO_2 adsorption on the surfaces of the pores. The parametrization is based on either density functional theory (DFT) or wave function theory (WFT) calculations.

DFT is applicable to larger systems than WFT, but the results are dependent on the choice of the functional. A particular functional may perform well for a specific system but may not be transferable to a different system. For that reason, it is important to validate the applicability of a specific functional for a specific property under study.

In contrast to DFT, WFT is a first-principles theory, functional- and parameter-free, but its applicability is limited to relatively small molecular systems. For example, coupled-cluster with iterative singles-and-doubles excitations and a perturbative treatment of triples excitations (CCSD(T)) provides accurate results, but only when the basis set is approaching the complete basis set (CBS) limit. The singles-and-doubles excitations have a N^6 scaling behavior, while the perturbative calculation of the triples needs a computational step of N^7, where N is the system size. The CBS limit needs very large basis sets (about quintuple-ζ quality or larger), which makes calculations of larger systems computationally unaffordable. This problem is known as slow convergence to the basis set limit.

Since the accurate computation of large molecular systems is of high interest, a huge number of approximate coupled-cluster methods have been proposed in recent decades.[27−56] The computational costs of these methods were reduced by different strategies, like the fragmentation of molecular orbitals,[31,32,57−59] the electrostatically embedded many-body expansion,[60−63] the natural linear scaling coupled-cluster,[30,38,64] the divide-and-conquer scheme,[41,65,66] the incremental scheme,[67−74] and the cluster-in-molecule method,[40,43,75−78] as well as Pulay-type local

Received: December 30, 2014

DOI: 10.1021/ct5011888
J. Chem. Theory Comput. XXXX, XXX, XXX−XXX

correlation methods.[27,28,79−84] The latter local correlation methods suffer from the so-called domain error, which may introduce discontinuities in the potential energy surface.[85] This discontinuity problem can be solved by merging the domains[86] or using bump functions.[33,34] It was recently shown that explicitly correlated F12 terms can be used to remove the domain error.[81,82]

In this work, accurate CCSD(T) calculations between CO_2 and functional groups of MOFs are presented for a quantitative understanding of the formation of CO_2 non-covalent interactions. We have chosen mainly polar organic linkers as functional groups based on MOFs which demonstrate very good behavior on CO_2 adsorption. In this study, no chemisorbed CO_2 nor adsorption on coordinatively unsaturated metal cations is taken into account. Crystalline effects which can also affect the binding affinity of CO_2, such as pore size and pore window size, are not considered in this work.

For the purpose of this study, we have developed a novel CCSD(T) scheme based on the incremental expansion of local domains,[36,87] which include interference effects from explicitly correlated theory.[88,89] The local nature of the incremental expansion[67] increases the applicability of accurate CCSD(T) calculations to larger molecular complexes, while the interference correction accelerates the convergence to the basis set limit of the method. The novel method is abbreviated as "inc-CCSD(T)|MP2+F12+INT". A brief description of these two theoretical concepts is given in section 2. Details about the incremental scheme[36,87,90−93] and the interference corrections[88,89,94] can be found in the original publications. The performance of the inc-CCSD(T)|MP2+F12+INT approach is tested on a set composed of 34 molecules (section 3.1).

Furthermore, the strength of interaction between CO_2 and common building blocks of MOFs is examined by means of the fragmentation scheme with interference effects. The set of 23 building blocks and the reasons that led us to include them in this study are discussed in section 3.2. For some building blocks, two different conformations with CO_2 are examined, yielding in total a set of 28 complexes. The good agreement between the inc-CCSD(T)|MP2+F12+INT scheme and some dispersion-corrected popular functionals is demonstrated in section 3.3. The two methodologies, which are based on different concepts, provide consistent results.

2. THEORETICAL ASPECTS

2.1. Incremental Scheme. In an incremental calculation, the total system is partitioned into disjoined sets of localized occupied orbitals—the one-site domains.[36,95,96] The total energy of a system can be computed on the basis of these domains using the incremental series in eq 1. For the first order, one computes the correlation energies for each domain separately and sums them. In order to correct for the non-additivity of the total energy, it is necessary to include pairs, triples, etc. of domains, until the desired accuracy is reached.[36,67] To avoid a double counting of correlation energy contributions, one has to subtract all permutations of lower order terms when computing an increment. The incremental series can be conveniently expressed using a set theory notation:

$$E_{\text{corr}} = \sum_{\mathbb{X}\in\mathcal{P}(\mathbb{D})\wedge|\mathbb{X}|\le O} \Delta\varepsilon_{\mathbb{X}} \tag{1}$$

where $\mathcal{P}(\mathbb{D})$ is the power set of the set of the domains $\mathbb{D}$. The restriction to the cardinality of the sets $\mathbb{X}$ truncates the incremental series at the desired order O. The general increment is defined as

$$\Delta\varepsilon_{\mathbb{X}} = \varepsilon_{\mathbb{X}} - \sum_{\mathbb{Y}\in\mathcal{P}(\mathbb{X})\wedge|\mathbb{Y}|<|\mathbb{X}|} \Delta\varepsilon_{\mathbb{Y}} \tag{2}$$

where $\varepsilon_{\mathbb{X}}$ is the correlation energy of the combined subsystems of $\mathbb{X}$. In order to make the scheme efficient, we neglect increments if the underlying one-site domains are spatially distant,[95,97] and we use a domain-specific basis set[91,98−101] to reduce the virtual space in the correlation calculations. The basic idea of this approximation is to divide the system into two regions when calculating the correlation energy of a domain. In the main region of a domain we use the large basis set, and in the environment we use a small unpolarized double-ζ basis set. It has been found in our previous work that the MP2 method can be effectively used to remove the basis set truncation error of the domain-specific basis set:

$$E_{\text{corr}}^{\text{inc}}(\text{CCSD(T)}) - [E_{\text{corr}}^{\text{inc}}(\text{MP2}) - E_{\text{corr}}(\text{MP2})] \tag{3}$$

To perform the statistical analysis of the errors ($\Delta_i = E_i^{\text{inc}} - E_i^{\text{ref}}$), we use

$$\text{the mean deviation:} \quad \mu = \frac{1}{n}\sum_{i=1}^{n}\Delta_i$$

$$\text{the standard deviation:} \quad \sigma = \sqrt{\frac{1}{n-1}\sum_{i=1}^{n}(\Delta_i - \mu)^2}$$

2.2. Interference Effects. The conventional CCSD(T) correlation energy at the basis set limit can be approximated as the sum between the CCSD(T) energy calculated from a truncated, small basis set (SB) and second-order correction terms. The second-order terms are typically obtained from the difference between MP2 energies calculated from two different basis sets, as follows:

$$E_{\text{CCSD(T)/CBS}}^{\text{corr}} \approx E_{\text{CCSD(T)}}^{\text{corr}} + (E_{\text{MP2/LB}}^{\text{corr}} - E_{\text{MP2/SB}}^{\text{corr}}) \tag{4}$$

where LB corresponds to a relatively large basis set. In eq 4, the MP2 basis set truncation error mimics the corresponding error of the CCSD(T) method. However, these two methods have a different convergence behavior toward the CBS limit. An alternative approach is to scale the MP2 truncation error by f_{ij}. The interference factor f_{ij} is computed from first-principles from the first-order Møller−Plesset wave function for individual electron pairs ij.[88,94] The MP2 truncation error is defined as the difference between the explicitly correlated MP2 (MP2-F12)[102] and conventional MP2 energies. When interference effects are added, the CCSD(T) energy at the basis set limit can be approximated as

$$E_{\text{CCSD(T)/CBS}} \approx E_{\text{CCSD(T)+F12+INT}} \tag{5}$$

$$= E_{\text{CCSD(T)}} + \delta E_{\text{F12}} + \delta E_{\text{INT}} + \delta E_{\text{CABS}} \tag{6}$$

$$\delta E_{\text{F12}} = \sum_{ij}(e_{ij}^{\text{MP2-F12}} - e_{ij}^{\text{MP2}}) \tag{7}$$

$$\delta E_{\text{INT}} = \sum_{ij}(f_{ij} - 1)(e_{ij}^{\text{MP2-F12}} - e_{ij}^{\text{MP2}}) \tag{8}$$

The notations δE and e_{ij} correspond to energy corrections and orbital pair energies, respectively. The term δE_{CABS} is a correction to the Hartree−Fock energy, obtained from single excitations to

DOI: 10.1021/ct5011888
J. Chem. Theory Comput. XXXX, XXX, XXX−XXX

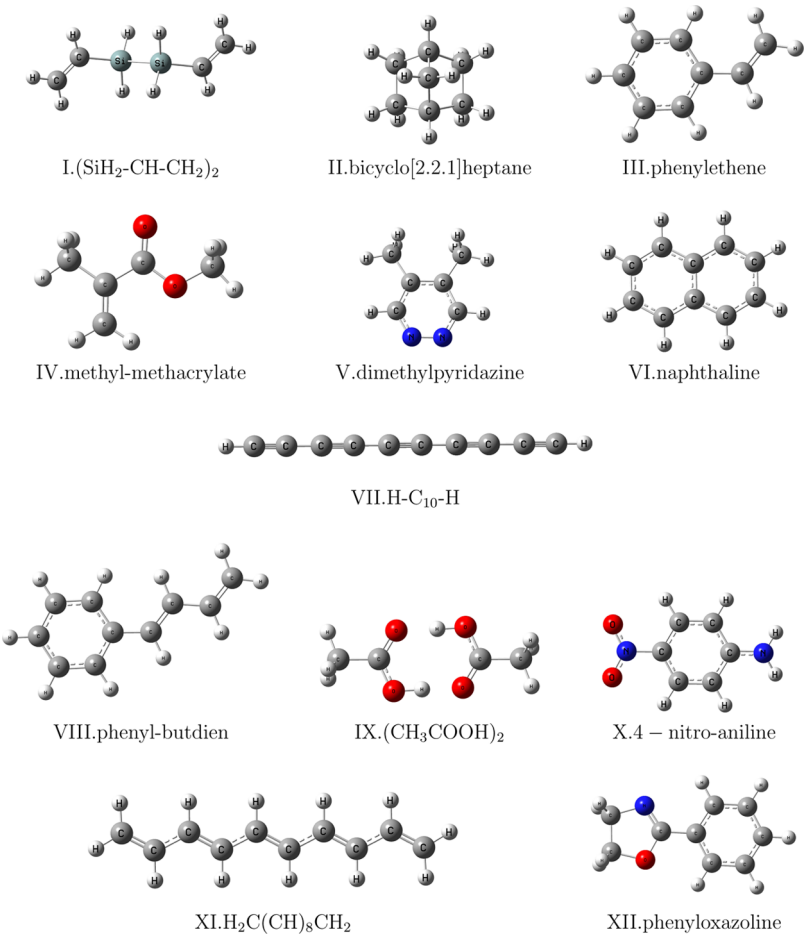

Figure 1. Structures of the molecules in the chosen test set (part I).

the complementary virtual space introduced by the explicitly correlated theory.[103] The CCSD(T)+F12+INT scheme has been used successfully for the accurate calculation of non-covalent interactions[104−106] and atomization energies.[89]

2.3. Computational Details. The coupled-cluster calculations were performed with a development version of the TURBOMOLE program package.[107]

In the environment of the increments,[93] the SV[108] basis set was used in combination with the appropriate RI basis set[109] for density fitting. The default input parameters were used for the incremental calculations, as proposed in ref 93. The truncation parameters[93,97] in the incremental series are t_{main} = 3 bohr, dsp = 4, and f = 30, where dsp is a measure of the number of occupied orbitals in a domain, i.e., it controls the size of the domain. The incremental series is truncated at third order in all calculations of this work. The required data, such as MO coefficients, overlap, overlap of two basis sets, and dipole integrals, were obtained from a modified version of the ricc2 module.[87] In the explicitly correlated calculations with interference effects, we used a Slater-type correlation factor as proposed by Ten-no.[110] In TURBOMOLE, the Slater-type function is represented by a linear combination of six Gaussians.[111] Furthermore, we applied the cc-pVDZ-F12 basis set of Peterson[112,113] using the corresponding CABS[114] and the recommended exponents in the correlation factor ($0.9a_0^{-1}$). The aug-cc-pVDZ basis set was used for Zn. For the Zn-containing compounds we used $1.4a_0^{-1}$ as exponent in the correlation factor and also for CO_2 in this case. The details of the explicitly correlated MP2-F12[102] computations are ansatz 2, approximation B,[115] and the fixed amplitude approach.[116]

The general test set used for the verification of the inc-CCSD(T)|MP2+F12+INT method was mainly taken from ref 92, with the addition of a few new structures. The corresponding geometries were optimized with the BP86/def2-TZVP[108,117−119] level of theory using the RI approximation as implemented in TURBOMOLE.[120−122] The obtained structures were characterized as minima by analyzing the Hessian matrix.[123]

Geometry optimizations at the BP86/def2-TZVPP level of theory[108,117−119] were carried for the 28-complex set of MOF building blocks interacting with CO_2. A second set of polarization functions was added for the correct description of the non-covalent interactions. Dispersion effects were added from the semi-empirical D3 correction of Grimme et al.[124] with the Becke−Johnson damping. The grid size for numerical integration was set to m4, and the structures were converged to a Cartesian gradient norm of 10^{-5} hartree/bohr. The stationary points where characterized by an analysis of the Hessian using numerical second derivatives.

The BP86/def2-TZVPP zero-point vibrational energy (ZPVE) was included in the binding energies.

3. RESULTS

3.1. General Test Set. In order to analyze the accuracy of our approach, we created a test set of 34 molecules with different electronic structures (Figures 1−2). The atom types in the test set were restricted to H, C, N, O, F, Mg, Si, S, and Cl. The

DOI: 10.1021/ct5011888
J. Chem. Theory Comput. XXXX, XXX, XXX−XXX

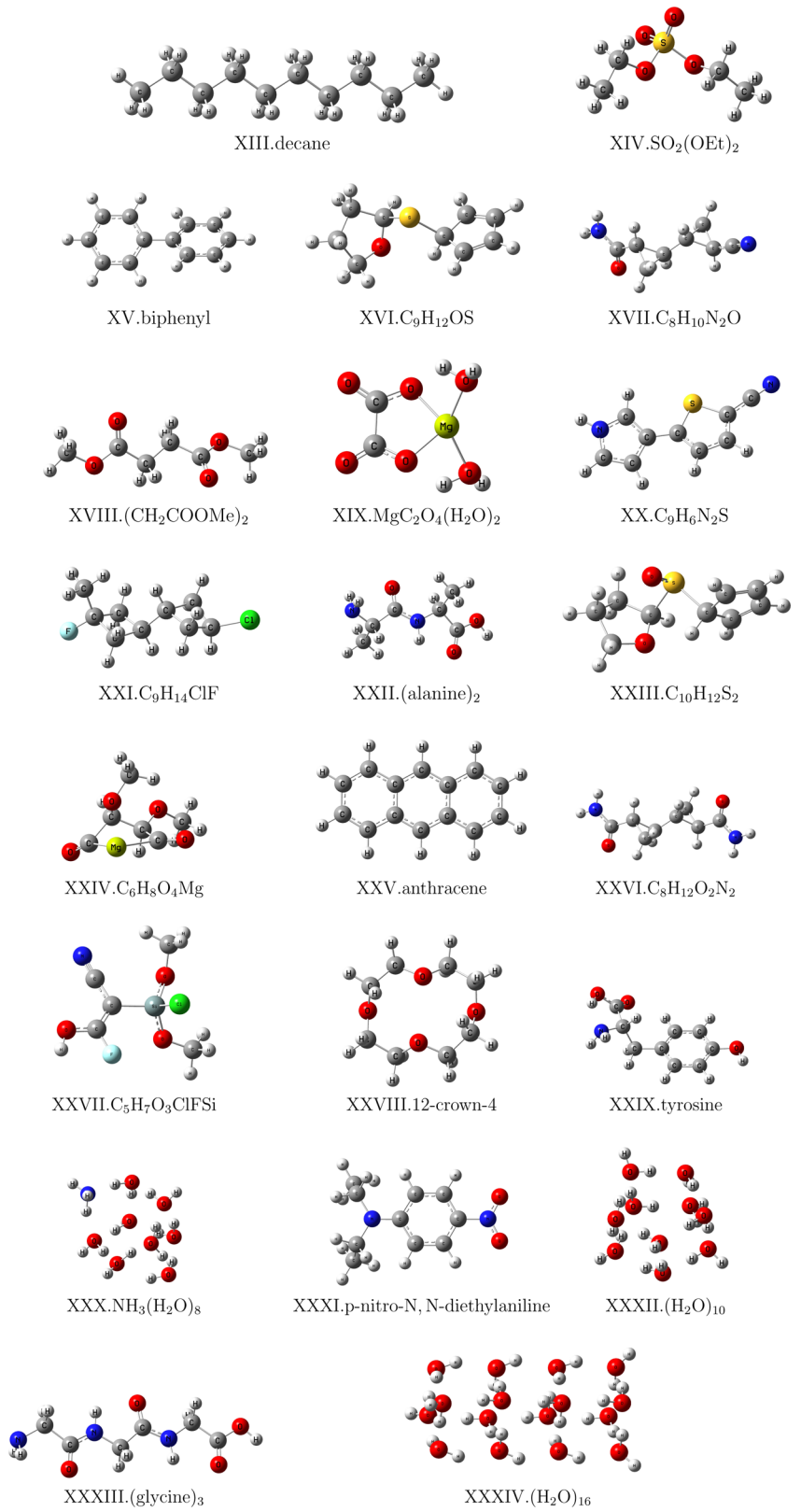

Figure 2. Structures of the molecules in the chosen test set (part II). The structure of the water decamer (XXXII) was taken from Piecuch and coworkers.[125] The structure of $(H_2O)_{16}$ (XXXIV) is taken from Yoo et al.[126] The structures of methyl methacrylate (IV) and phenyloxazoline (XII) were optmized with the PBE0 functional as in ref 127.

complete set of data is given in the Supporting Information. Here we briefly analyze the errors of the most important statistical measures. In Figure 3 we present the errors of the incremental expansions for MP2 and CCSD(T), as well as for MP2-corrected incremental CCSD(T) (eq 3). Since the interference factors and the MP2-F12 terms are not computationally demanding, we

DOI: 10.1021/ct5011888
J. Chem. Theory Comput. XXXX, XXX, XXX−XXX

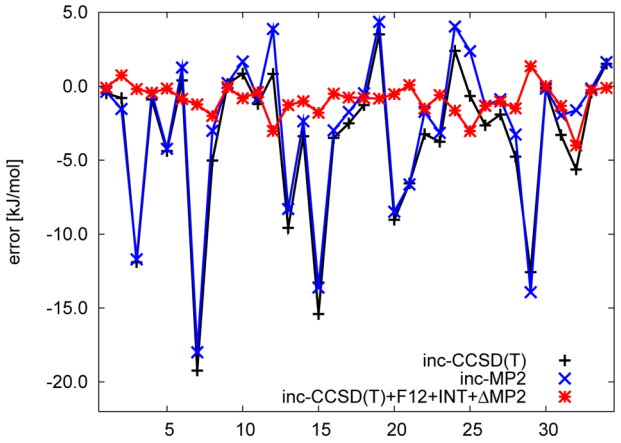

Figure 3. Errors in the absolute energies due to the local approximations for different quantum chemical methods. The error of MP2 is very similar to the CCSD(T) error for all molecules; therefore, one can use MP2 to correct the incremental CCSD(T) energies. For the names of the molecules, refer to Figures 5−7.

computed them without local approximations. Therefore, the error of the inc-CCSD(T)|MP2+F12+INT method is the same as the error of inc-CCSD(T)|MP2. The systems are ordered on the basis of the increasing magnitude of the CCSD(T) correlation energy, and the numbering is the same as in Figures 1−2. When considering the incremental MP2 and CCSD(T) expansions, we see that the errors are quite similar. Based on this finding, we can use the computationally less demanding MP2 method to reduce the error of the coupled-cluster calculations. Considering the red CCSD(T)|MP2+F12+INT curve, we see very small errors for all systems in our test set. In Figure 4 we

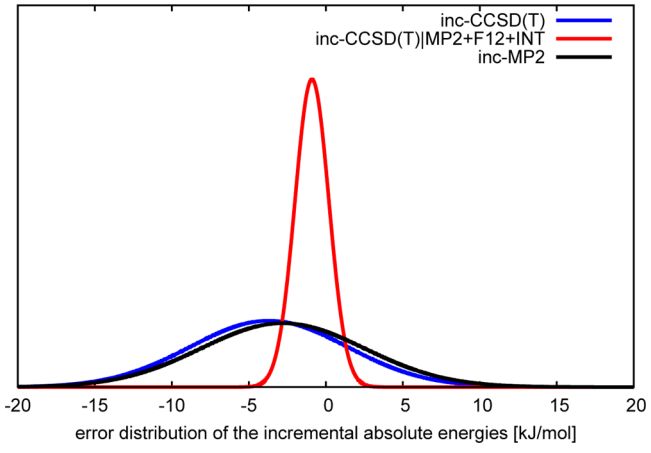

Figure 4. Error distributions for incremental MP2 and coupled-cluster. We assume that the errors are Gaussian distributed. The MP2 correction improves the accuracy of the scheme significantly. Lowest deviations from the reference values are reached at the inc-CCSD(T)|MP2+F12+INT level.

compare the errors due to the local approximations using Gaussian distributions. In Table 1 we demonstrate the accuracy of the novel method (inc-CCSD(T)|MP2+F12+INT) for approximating the absolute energies of the parent method using the mean (μ) and the standard deviation (σ).

3.2. CO_2 Adsorption. The non-covalent interactions of CO_2 with building blocks of MOFs have been examined with the interference-corrected incremental scheme. A set of 22 organic

Table 1. Statistical Errors Due to the Local Approximations for the Absolute Energies of Different Electronic Structure Methods (in kJ/mol)

method	MP2	CCSD(T)	inc-CCSD(T)|MP2+F12+INT
μ	−2.8	−3.7	−0.9
σ	5.3	5.1	1.1

molecules was compiled for the purposes of this study (Figures 5−7). The majority of the structures in this study have already been used in the synthesis or post-modification of MOFs. In addition, basic zinc acetate (Figure 7), an inorganic building unit which is present in a large variety of hybrid frameworks,[128,129] is also included. All structures were optimized at the DFT (BP86-D3/def2-TZVPP) level of theory. Two energetically comparable minima were found for 5 complexes out of 23, forming in total a set of CO_2 complexes composed of 28 structures (Figures 5−7). The names of the building units, the chemical formulas, the abbreviations used in this article, and the strengths of the non-covalent interaction energies with CO_2 are listed in Table 2.

The 28 complexes can be separated on the basis of the functional group that interacts with CO_2. These are amino-,[128,130,131] chloro-,[132] cyano-,[132] and NO_2-functionalized[132] building blocks and nitrogen-containing[5,14,133,134] or azo-bridged[135,136] units. In some specific cases, DFT geometry optimizations predict a more favorable aromatic $\pi-CO_2$ interaction than a direct interaction with the functional group. These cases are included in Table 2 as "aromatic ring"-type interactions as, for example, in the Cl- and CF_3-functionalized units of **22.cbIm-1** and **26.pycf3-2**, respectively. Similarly, the **4.dpt** and **5.bdpd** N-containing molecules have more favorable $\pi-CO_2$ interactions than the coplanar geometry. In a previous study,[20] we have seen that the coplanar geometry is more favorable for complexes of CO_2 with N-heteroaromatic molecules. We should clarify that the coplanar geometry was not taken under consideration in cases where the N atom of the organic linker is coordinated to the metal centers of MOF materials and, thus, is not accessible to the gas molecules. For example, the coplanar conformation of CO_2 with the N atoms of the pyridine and pyrazole groups of **4.dpt** and **5.bdpd**, respectively, is not included in this study. On the contrary, the coplanar conformation of CO_2 with the 1,2,4,5-tetrazine core of **4.dpt** was examined. However, the H atoms of the pyridine group hinder the formation of this conformation; thus, the DFT optimized geometry predicts a more stable $\pi-CO_2$ complex.

For the sake of completeness, the non-functional **1.bdc** and **3.btc** organic linkers, common blocks in a wide variety of MOFs,[128,129] are included in this study. Molecules that contain carboxylate groups are terminated with Li^+ cations, which give a better representation of the cationic, inorganic building blocks.[137] The difference in the CO_2 interaction energies between the Li^+-terminated **2.bdc-li** and the carboxylic acid analogue **1.bdc** is about 1.6 kJ/mol.

The size of the molecular complexes in Figures 5−7 varies between 10 and 33 non-hydrogen atoms. The largest complexes considered in this study are the **27.zn4o-1**, **28.zn4o-2**, and **18.abtc** cases, which include 32, 32, and 33 non-hydrogen atoms, respectively.

The highest CO_2 affinity is observed for the nitrogen heterocycles **9.pur** and **10.ade**, with CCSD(T) interaction energies of −22.4 and −23.4 kJ/mol, respectively. The nature of this interaction is characterized by electron donation from the lone pair of the nitrogen to the carbon of CO_2. Hydrogen bonds

DOI: 10.1021/ct5011888
J. Chem. Theory Comput. XXXX, XXX, XXX−XXX

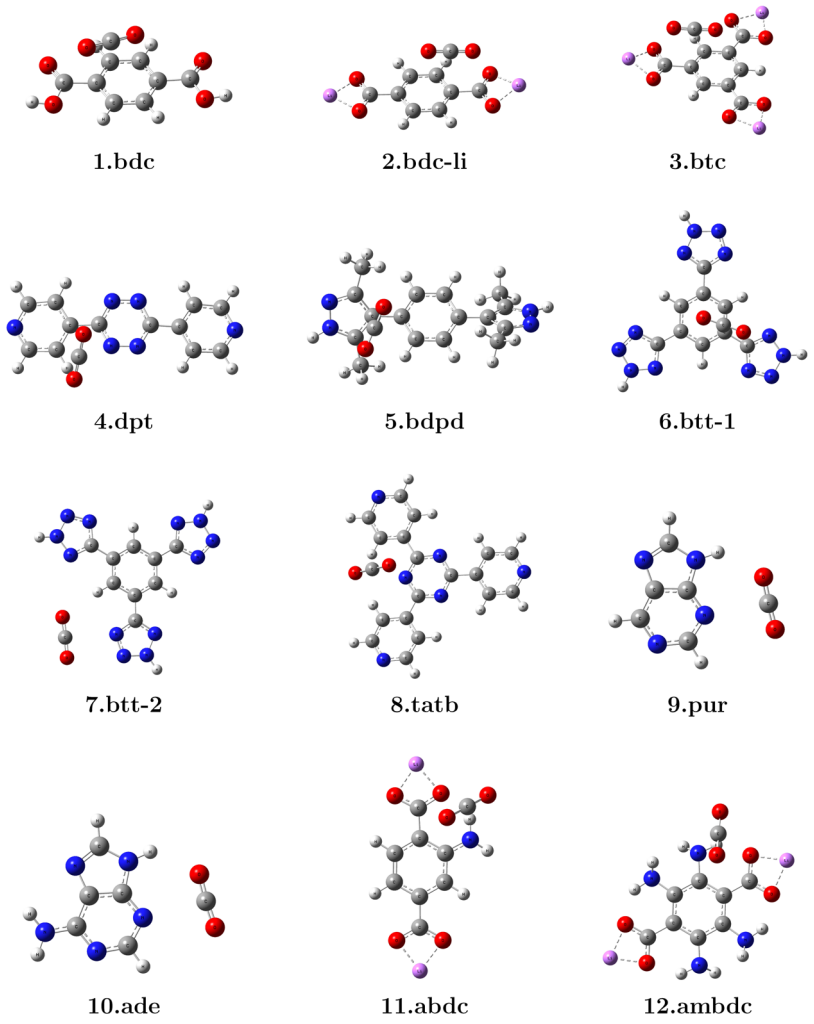

Figure 5. DFT optimized structures of building units of MOFs with CO_2 used in this study (part I).

between the oxygen of CO_2 and the hydrogen of the five-membered ring stabilize this molecular configuration further. Microwave spectroscopy has verified that the global minimum-energy structure of the pyridine−CO_2 complex is indeed the coplanar configuration.[138] The pyridine−CO_2 complex shares some similarities with the **9.pur** and **10.ade** complexes. The main difference is the strength of interaction; the purine-type molecules interact more strongly with the CO_2 molecule than the pyridine-type ones.[20] The remaining two N-heterocycle complexes (**7.btt-2** and **8.tatb**) show a significantly lower binding energy for CO_2. For the case of **8.tatb**, the two hydrogens of the pyridine rings hinder the formation of the coplanar geometry with the triazine ring. In contrast, **7.btt-2** possesses three tetrazole rings which do not bind CO_2 as strongly as the purine-type heterocycles.[20] In addition, the tetrazole rings are coordinated with the metal cations of the MOFs; thus, they are not fully accessible to the gas molecules.

The interaction of CO_2 with amine-functionalized and azo-linkage groups is weaker than that with the N-containing heterocycles but is still in an energy range (−13.2 to −17.1 kJ/mol) for enhanced CO_2 uptake in practical applications.[8−13] The carbon atom of CO_2 binds to the lone pair of the nitrogen in the $-NH_2$ group for all amine-type building blocks listed in Table 2. Infrared spectroscopy has elucidated this type of interaction between $-NH_2$ groups and CO_2.[139] The only exception is the **13.diamino**−CO_2 complex, where the CO_2 molecule is located farther from the $-NH_2$ group and closer to the aromatic ring. The complexes are further stabilized by hydrogen bonds between one of the oxygens of CO_2 and the hydrogen of the amino group. For the amino-functionalized aromatic cases (**11.abdc**, **12.ambdc**, and **13.diamino**), the O···H distances are 2.85, 2.86, and 2.86 Å, respectively, while for the remaining three complexes the O···H distances are between 3.15 and 3.32 Å. Similarly, CO_2 forms a non-covalent bond with the azo bridge of **17.azpy** and **18.abtc** (C···N distance at 2.98 and 3.00 Å, respectively), and the final geometries are stabilized by C−H···O hydrogen bonds between 2.75 and 3.02 Å. This type of interaction has a strength of approximately −16.9 kJ/mol.

The organic molecules involved in the complexes **19.cnIm**, **20.nIm**, **21.nbIm**, **22.cbIm-1**, and **23.cbIm-2** have been used for the synthesis of isoreticular zeolitic imidazolate frameworks (ZIFs).[132] From this series of MOFs, ZIF-78, ZIF-82, and ZIF-94[140] show the highest affinity for CO_2 when compared to other isoreticular ZIFs. ZIF-78 and ZIF-82 include the **21.nbIm** and **19.cnIm** linkers, respectively. **21.nbIm** possesses NO_2 as a functional group, and **19.cnIm** has a CN group. The interaction energy between these functional groups is approximately −13.5 kJ/mol, as predicted from the inc-CCSD(T)|MP2+F12+INT level of theory. These energies are in agreement with the binding energies reported by Morris et al.[140] From their molecular simulations, they concluded that different adsorption sites bind CO_2 in ZIFs. For sites surrounded by the imidazolate linkers,

DOI: 10.1021/ct5011888
J. Chem. Theory Comput. XXXX, XXX, XXX−XXX

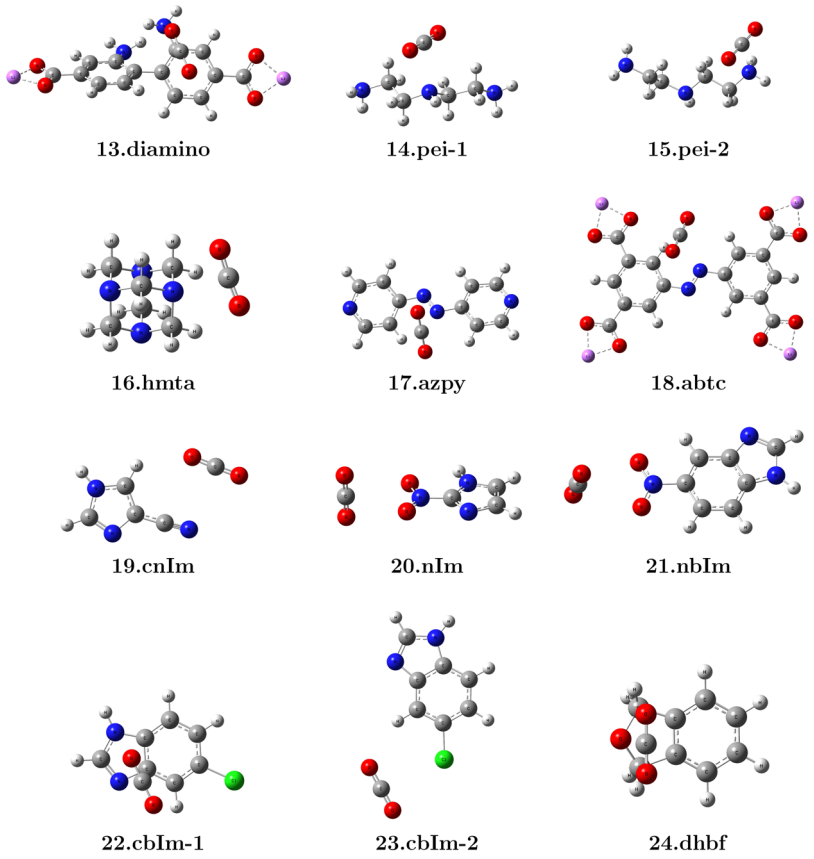

Figure 6. DFT optimized structures of building units of MOFs with CO_2 used in this study (part II).

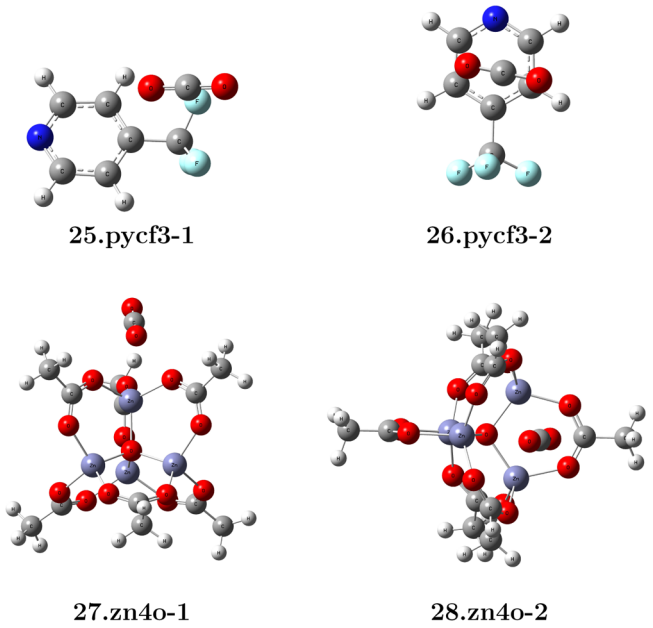

Figure 7. DFT optimized structures of building units of MOFs with CO_2 used in this study (part III).

they predict a binding energy of −14.3 kJ/mol. However, the binding affinity of CO_2 in the pore corners or in the framework channels is dramatically increased by up to −40.6 kJ/mol due to cooperative effects within the ring of six or eight zincs, interactions between multiple functional groups of the linkers, or combination of both.

From the remaining complexes in Table 2, **24.dhbf** shows a CO_2 interaction strength (−13.6 kJ/mol) comparable to that of the amine-type linkers. This building block has been suggested by Babarao et al.[141] for functionalizing porous aromatic frameworks. From their grand canonical Monte Carlo (GCMC) simulations, they concluded that this enhanced material has higher CO_2 storage capacity at low pressures. In contrast, Cl- or CF_3-containing molecules do not increase the strength of the CO_2 interaction compared to N-heterocycle-, amine-, or azo-bridged linkers. For both Cl- and CF_3-containing molecules, the aromatic site interacts more strongly with CO_2 than the functional group, and it has been assigned as the primary binding site. Both DFT geometry optimizations for **22.cbIm-1** and **26.pycf3-2** complexes, which are characterized as "aromatic ring"-type interactions, have started from a $-Cl\cdots CO_2$ and $-CF_3\cdots CO_2$ initial conformation, respectively. The relaxed geometries (Figures 6 and 7) verified that the functional group can be considered as a secondary binding site. Additional conclusions may be extracted from the out-of-plane conformation of CO_2 with the 4-(trifluoromethyl)pyridine molecule (**26.pycf3-2**). Comparison between this out-of-plane complex and the corresponding pyridine$-CO_2$ complex reveals that the electron-withdrawing CF_3 group reduces the strength of the interaction. Chen et al.[142] have estimated the out-of-plane CCSD(T)/CBS interaction energy between pyridine and CO_2 at −10.5 kJ/mol. This energy is 0.8 kJ/mol lower than the one we obtain for **26.pycf3-2**.

It should be mentioned that all complexes included in this study are considered in their neutral form. However, some of these linkers, such as complexes **19**−**23**, are deprotonated at the imidazole N−H sites to bind metals during the formation of

DOI: 10.1021/ct5011888
J. Chem. Theory Comput. XXXX, XXX, XXX−XXX

Table 2. List of Building Units of MOFs Included in This Study (Name, Chemical Formula, and Abbreviation Used in Text), CO_2 Interaction Energies E_{Int} (in kJ/mol) Calculated from the Incremental CCSD(T) Scheme with Interference Effects at the BP86/def2-TZVPP Optimized Structures (Figures 5−7), and Their Functional Group Interacting with CO_2[a]

abbreviation	name	formula	interacting group	E_{Int}
1.bdc	benzene dicarboxylate	$C_8H_6O_4$	aromatic ring	−11.3
2.bdc-li	benzene dicarboxylate (terminated with Li)	$C_8H_4O_4Li_2$	aromatic ring	−12.9
3.btc	benzene tricarboxylate	$C_9H_3O_6Li_3$	aromatic ring	−11.6
4.dpt	1,2,4,5-tetrazine-3,6-dipyridyl	$C_{12}H_8N_6$	aromatic ring	−6.9
5.bdpd	1,4-bis[(3,5-dimethyl)-pyrazol-4-yl]benzene	$C_{16}H_{18}N_4$	aromatic ring	−15.3
6.btt-1	1,3,5-benzenetristetrazolate	$C_9H_6N_{12}$	aromatic ring	−14.0
7.btt-2	1,3,5-benzenetristetrazolate (2)	$C_9H_6N_{12}$	N-heterocycle	−13.0
8.tatb	4,4′,4″-*s*-triazine-2,4,6-triyltribenzoate	$C_{15}H_{12}N_6$	N-heterocycle	−8.4
9.pur	purine	$C_5H_4N_4$	N-heterocycle	−22.4
10.ade	adenine	$C_5H_5N_5$	N-heterocycle	−23.4
11.abdc	2-aminoterephthalic acid	$C_8H_5O_4NLi_2$	amine	−17.1
12.ambdc	amino-functionalized benzene dicarboxylate	$C_8H_8O_4N_4Li_2$	amine	−14.9
13.diamino	2,2′-diaminobiphenyl-4,4′-dicarboxylic acid	$C_{14}H_{10}O_4N_2Li_2$	amine	−13.2
14.pei-1	polyethylenimine	$C_4H_{13}N_3$	amine	−15.8
15.pei-2	polyethylenimine (2)	$C_4H_{13}N_3$	amine	−13.7
16.hmta	hexamethylenetetramine	$C_6H_{12}N_4$	Amine	−15.8
17.azpy	*trans*-4,4′-azodipyridine	$C_{10}H_8N_4$	azo linkage	−17.0
18.abtc	3,3′,5,5′-azobenzenetetracarboxylate	$C_{16}H_6O_8N_2Li_4$	azo linkage	−16.8
19.cnIm	4-cyano-1*H*-imidazole	$C_4H_3N_3$	CN group	−13.5
20.nIm	2-nitro-1*H*-imidazole	$C_3H_3O_2N_3$	NO_2 group	−13.5
21.nbIm	6-nitro-1*H*-benzimidazole	$C_7H_5O_2N_3$	NO_2 group	−13.3
22.cbIm-1	6-chloro-1*H*-benzimidazole	$C_7H_5N_2Cl$	aromatic ring	−12.6
23.cbIm-2	6-chloro-1*H*-benzimidazole (2)	$C_7H_5N_2Cl$	Cl atom	−6.3
24.dhbf	1,3-dihydro-2-benzofuran	$C_8H_8O_2$	dihydrobenzofuran	−13.6
25.pycf3-1	4-(trifluoromethyl)pyridine	$C_6H_4NF_3$	CF_3 group	−5.3
26.pycf3-2	4-(trifluoromethyl)pyridine (2)	$C_6H_4NF_3$	aromatic ring	−9.8
27.zn4o-1	basic zinc acetate	$C_{12}H_{18}O_{13}Zn_4$	Zn_4O	−19.1
28.zn4o-2	basic zinc acetate (2)	$C_{12}H_{18}O_{13}Zn_4$	Zn_4O	−21.7

[a]The ZPVE is included at the BP86-D3/def2-TZVPP level of theory. In the interacting groups, "N-heterocycle" corresponds to structures where CO_2 interacts directly with the N atom of the heteroaromatic molecule. Cases that include N atoms in their aromatic ring but have CO_2 located above the level of the ring are categorized as "aromatic ring".

MOFs or ZIFs. Thus, a delocalized electron density is expected, which may affect the CO_2 binding affinity. This delocalization will have a direct impact on five-membered rings, such as **19.cnIm** and **20.nIm**. For a more in-depth analysis, molecular models that incorporate the metal building blocks should be examined by means of electronic structure theory. The consequences of these effects can be the topic of a separate study.

Finally, to test the applicability of the inc-CCSD(T)|MP2+F12+INT scheme, the CO_2 interaction with basic zinc acetate (**27.zn4o-1** and **27.zn4o-2**) was examined. This complex has in total 32 non-hydrogen atoms, 29 from the inorganic building block plus the 3 from the CO_2 molecule, which constitutes a challenging case for CCSD(T). Two different CO_2 binding sites were taken into account, with interaction energies of −19.1 and −21.7 kJ/mol. In the real environment of a material that contains this inorganic building block (e.g., MOF-5[129]), the binding site of the **27.zn4o-1** complex is stereochemically less favorable for CO_2 adsorption. On the contrary, GCMC simulations[143] predict that the **27.zn4o-2** binding site is the most favorable for CO_2 adsorption on MOF-5. From the classical mechanics study of Dubbeldam et al.,[143] a binding energy of −22.2 kJ/mol was reported, which is only 0.5 kJ/mol lower than the one obtained from our CCSD(T) scheme. A CO_2 positioned above the organic linker (benzenedicarboxylate) was assigned as a secondary site of MOF-5. The minimized classical energy for this site (−13.3 kJ/mol) is in very good agreement with the one found for **2.bdc-li** (−12.9 kJ/mol).

3.3. Comparison with DFT-D3. In Table 3, we compare the inc-CCSD(T)|MP2+F12+INT binding energies with those of popular density functionals using Grimme's D3 correction for dispersion effects. In general there is a very good agreement between the DFT results and our coupled-cluster energy. There are a few systems with larger differences up to 6.4 kJ/mol. When considering our σ of 1.1 kJ/mol for the absolute energies, we could end up in the unfavorable case that one reactant is 3σ too low and the other one is 3σ too high. Using this conservative estimate, our error interval for 99.7% confidence is 6σ, which corresponds to 6.6 kJ/mol. Based on these conservative considerations, we can conclude that the DFT-D3 results agree very well with our coupled-cluster results and that both methods are suitable tools to investigate such weakly interacting systems.

In general it is very important to have different computational models, based on different approximations, when computing chemical reactions. If the results of the calculations agree well, it is a strong indication that the theoretical value is correct, since it is unlikely that conceptually different approaches have the same error.

4. CONCLUSIONS

In this article, we report the performance of a novel and accurate coupled-cluster scheme which can be applied to relatively large

DOI: 10.1021/ct5011888
J. Chem. Theory Comput. XXXX, XXX, XXX−XXX

Table 3. DFT Interaction Energies (in kJ/mol) Using the D3 Dispersion Correction and the def2-TZVPP Basis Set[a]

system	PBE0-D3	TPSSH-D3	B3LYP-D3	BP86-D3	PW6B95-D3	TPSS-D3	CC
1.bdc	−10.0	−9.2	−10.2	−10.1	−9.9	−9.4	−11.3
2.bdc-li	−13.1	−12.2	−13.5	−13.4	−13.0	−12.4	−12.9
3.btc	−13.7	−12.9	−14.2	−14.2	−13.4	−13.0	−11.6
4.dpt	−9.3	−9.7	−10.2	−13.0	−8.9	−11.3	−6.9
5.bdpd	−16.9	−15.9	−17.5	−17.8	−17.4	−16.0	−15.3
6.btt-1	−11.9	−11.2	−12.4	−12.4	−11.7	−11.4	−14.0
7.btt-2	−12.7	−11.2	−12.7	−10.5	−12.2	−11.1	−13.0
8.tatb	−15.5	−14.6	−16.7	−16.4	−14.8	−14.8	−8.4
9.pur	−21.2	−19.2	−22.0	−20.1	−20.1	−18.9	−22.4
10.ade	−22.9	−20.8	−23.6	−21.9	−21.7	−20.5	−23.4
11.abdc	−16.6	−15.5	−18.0	−17.0	−17.9	−15.4	−17.1
12.ambdc	−18.4	−17.2	−19.8	−19.0	−19.2	−17.2	−14.9
13.diamino	−14.0	−13.2	−14.5	−15.5	−13.9	−13.5	−13.2
14.pei-1	−17.9	−17.1	−18.5	−19.2	−16.4	−17.5	−15.8
15.pei-2	−16.0	−14.9	−16.2	−15.7	−14.8	−15.1	−13.7
16.hmta	−17.2	−16.3	−17.7	−17.6	−14.6	−16.5	−15.8
17.azpy	−13.0	−12.1	−13.6	−13.8	−12.5	−12.5	−17.0
18.abtc	−16.4	−16.0	−17.4	−17.7	−15.9	−16.5	−16.8
20.nIm	−11.6	−10.7	−12.2	−10.5	−12.4	−10.9	−13.5
19.cnIm	−13.1	−11.9	−13.5	−11.3	−12.9	−11.8	−13.5
21.nbIm	−13.1	−12.0	−13.8	−11.9	−13.9	−12.0	−13.3
22.cbIm-1	−13.1	−12.1	−13.5	−13.1	−13.4	−12.2	−12.6
23.cbIm-2	−8.5	−7.6	−9.0	−7.5	−8.2	−7.7	−6.3
24.dhbf	−14.3	−13.2	−15.8	−15.0	−15.0	−13.3	−13.6
25.pycf3-1	−7.5	−7.3	−7.7	−6.0	−7.9	−7.7	−5.3
26.pycf3-2	−9.8	−9.3	−9.9	−9.4	−9.6	−9.5	−9.8
27.zn4o-1	−19.0	−17.6	−21.1	−19.1	−18.5	−17.4	−19.1
28.zn4o-2	−21.1	−20.5	−24.5	−23.5	−23.9	−20.2	−21.7

[a]The energies were obtained as single-point energies at the BP86-D3 structures. The BP86/def2-TZVPP ZPVE is included in all interaction energies. For the CC, inc-CCSD(T)|MP2+F12+INT/cc-pVDZ-F12, aug-cc-pVDZ for Zn and $\gamma = 1.4a_0^{-1}$ in these cases.

complexes. It is based on an incremental expansion of the total system into local domains with interference effects that accelerate the convergence of coupled-cluster theory to the basis set limit. This scheme has been applied to a study of non-covalent interactions of CO_2 with different types of organic building units of MOFs. Nitrogen-containing heteroaromatics have a higher affinity for CO_2 when compared to the complexes considered here. Other promising candidates for stronger CO_2 binding are amine-functionalized units and azo-bridged organic linkers. Dihydrobenzofuran can also be used as an alternative building block for the enhancement of the CO_2 sorption on MOFs. Furthermore, results from DFT-D3 are, in general, in good agreement with our approximate coupled-cluster scheme. This agreement makes us confident about the level of accuracy that our novel scheme can reach; it is very unlikely that both approximations break down at the same time with the same error.

■ ASSOCIATED CONTENT

Supporting Information

DFT energies, absolute correlation energies (in hartrees), and geometry coordinates for the test sets presented here. This material is available free of charge via the Internet at http://pubs.acs.org.

■ AUTHOR INFORMATION

Corresponding Author

*Fax: +49 (0) 371 531-839415. E-mail: joachim.friedrich@chemie.tu-chemnitz.de.

Funding

J.F. thanks the Fonds der Chemischen Industrie for financial support from the Material Cost Allowances program.

Notes

The authors declare no competing financial interest.

■ ACKNOWLEDGMENTS

The authors thank Prof. Hani El-Kaderi, Joshua Borycz, and Emmanuel Haldoupis for helpful discussions.

■ REFERENCES

(1) Ma, S.; Zhou, H.-C. *Chem. Commun.* **2010**, *46*, 44−53.
(2) Li, J.-R.; Ma, Y.; McCarthy, M. C.; Sculley, J.; Yu, J.; Jeong, H.-K.; Balbuena, P. B.; Zhou, H.-C. *Coord. Chem. Rev.* **2011**, *255*, 1791−1823.
(3) Sumida, K.; Rogow, D. L.; Mason, J. A.; McDonald, T. M.; Bloch, E. D.; Herm, Z. R.; Bae, T.-H.; Long, J. R. *Chem. Rev.* **2012**, *112*, 724−781.
(4) Liu, J.; Thallapally, P. K.; McGrail, B. P.; Brown, D. R.; Liu, J. *Chem. Soc. Rev.* **2012**, *41*, 2308−2322.
(5) Sumida, K.; Horike, S.; Kaye, S. S.; Herm, Z. R.; Queen, W. L.; Brown, C. M.; Grandjean, F.; Long, G. J.; Dailly, A.; Long, J. R. *Chem. Sci.* **2010**, *1*, 184−191.
(6) Zhou, D.-D.; He, C.-T.; Liao, P.-Q.; Xue, W.; Zhang, W.-X.; Zhou, H.-L.; Zhang, J.-P.; Chen, X.-M. *Chem. Commun.* **2013**, *49*, 11728−11730.
(7) Li, J.-R.; Yu, J.; Lu, W.; Sun, L.-B.; Sculley, J.; Balbuena, P. B.; Zhou, H.-C. *Nature Commun.* **2013**, *4*, 1538.
(8) Couck, S.; Denayer, J. F. M.; Baron, G. V.; Remy, T.; Gascon, J.; Kapteijn, F. *J. Am. Chem. Soc.* **2009**, *131*, 6326−6327.
(9) Vaidhyanathan, R.; Iremonger, S. S.; Shimizu, G. K. H.; Boyd, P. G.; Alavi, S.; Woo, T. K. *Science* **2010**, *330*, 650−653.

DOI: 10.1021/ct5011888
J. Chem. Theory Comput. XXXX, XXX, XXX−XXX

(10) Panda, T.; Pachfule, P.; Chen, Y.; Jiang, J.; Banerjee, R. *Chem. Commun.* **2011**, *47*, 2011−2013.
(11) Si, X.; Jiao, C.; Li, F.; Zhang, J.; Wang, S.; Liu, S.; Li, Z.; Sun, L.; Xu, F.; Gabelica, Z.; Schick, C. *Energy Environ. Sci.* **2011**, *4*, 4522−4527.
(12) Khutia, A.; Janiak, C. *Dalton Trans.* **2014**, *43*, 1338−1347.
(13) Yin, H.; Wang, J.; Xie, Z.; Yang, J.; Bai, J.; Lu, J.; Zhang, Y.; Yin, D.; Lin, J. Y. S. *Chem. Commun.* **2014**, *50*, 3699−3701.
(14) An, J.; Geib, S.; Rosi, N. L. *J. Am. Chem. Soc.* **2010**, *132*, 38−39.
(15) Lin, J.-B.; Zhang, J.-P.; Chen, X.-M. *J. Am. Chem. Soc.* **2010**, *132*, 6654−6656.
(16) Wang, X.-J.; Li, P.-Z.; Liu, L.; Zhang, Q.; Borah, P.; Wong, J. D.; Chan, X. X.; Rakesh, G.; Li, Y.; Zhao, Y. *Chem. Commun.* **2012**, *48*, 10286−10288.
(17) Lin, L.-C.; Berger, A. H.; Martin, R. L.; Kim, J.; Swisher, J. A.; Jariwala, K.; Rycroft, C. H.; Bhown, A. S.; Deem, M. W.; Haranczyk, M.; Smit, B. *Nat. Mater.* **2012**, *11*, 633−641.
(18) Altarawneh, S.; Behera, S.; Jena, P.; El-Kaderi, H. M. *Chem. Commun.* **2014**, *50*, 3571−3574.
(19) Li, P.-Z.; Wang, X.-J.; Zhang, K.; Nalaparaju, A.; Zou, R.; Zou, R.; Jiang, J.; Zhao, Y. *Chem. Commun.* **2014**, *50*, 4683−4685.
(20) Vogiatzis, K. D.; Mavrandonakis, A.; Klopper, W.; Froudakis, G. E. *ChemPhysChem* **2009**, *10*, 374−383.
(21) Altarsha, M.; Ingrosso, F.; Ruiz-Lopez, M. *ChemPhysChem* **2012**, *13*, 3397−3403.
(22) Azofra, L. M.; Altarsha, M.; Ruiz-Lopez, M. F.; Ingrosso, F. *Theor. Chem. Acc.* **2013**, *132*, 1326.
(23) Frysali, M. G.; Klontzas, E.; Froudakis, G. E. *ChemPhysChem* **2014**, *15*, 905−911.
(24) Düren, T.; Bae, Y.-S.; Snurr, R. Q. *Chem. Soc. Rev.* **2009**, *38*, 1237−1247.
(25) Borycz, J.; Lin, L.-C.; Bloch, E. D.; Kim, J.; Dzubak, A. L.; Maurice, R.; Semrouni, D.; Lee, K.; Smit, B.; Gagliardi, L. *J. Phys. Chem. C* **2014**, *118*, 12230−12240.
(26) Li, W.; Shi, H.; Zhang, J. *ChemPhysChem* **2014**, *15*, 1772−1778.
(27) Hampel, C.; Werner, H.-J. *J. Chem. Phys.* **1996**, *104*, 6286−6297.
(28) Schütz, M.; Hetzer, G.; Werner, H. J. *J. Chem. Phys.* **1999**, *111*, 5691−5705.
(29) Schütz, M. J. *Chem. Phys.* **2000**, *113*, 9986−10001.
(30) Flocke, N.; Bartlett, R. J. *J. Chem. Phys.* **2004**, *121*, 10935−6003.
(31) Fedorov, D. G.; Kitaura, K. *J. Chem. Phys.* **2004**, *121*, 2483−2490.
(32) Fedorov, D. G.; Kitaura, K. *J. Chem. Phys.* **2005**, *123*, 134103.
(33) Subotnik, J. E.; Head-Gordon, M. *J. Chem. Phys.* **2005**, *123*, 64108.
(34) Subotnik, J. E.; Sodt, A.; Head-Gordon, M. *J. Chem. Phys.* **2006**, *125*, 074116.
(35) Auer, A.; Nooijen, M. *J. Chem. Phys.* **2006**, *125*, 024104.
(36) Friedrich, J.; Hanrath, M.; Dolg, M. *J. Chem. Phys.* **2007**, *126*, 154110.
(37) Mata, R. A.; Werner, H.-J.; Schütz, M. *J. Chem. Phys.* **2008**, *128*, 144106.
(38) Hughes, T. F.; Flocke, N.; Bartlett, R. J. *J. Phys. Chem. A* **2008**, *112*, 5994−6003.
(39) Herrmann, A.; Schwerdtfeger, P. *Phys. Rev. Lett.* **2008**, *101*, 183005.
(40) Li, W.; Piecuch, P.; Gour, J. R.; Li, S. *J. Chem. Phys.* **2009**, *131*, 114109.
(41) Kobayashi, M.; Nakai, H. *J. Chem. Phys.* **2009**, *131*, 114108.
(42) Gordon, M. S.; Mullin, J. M.; Pruitt, S. R.; Roskop, L. B.; Slipchenko, L. V.; Boatz, J. A. *J. Phys. Chem. B* **2009**, *113*, 9646−9663.
(43) Li, W.; Piecuch, P. *J. Phys. Chem. A* **2010**, *114*, 6721−6727.
(44) Schwerdtfeger, P.; Assadollahzadeh, B.; Herrmann, A. *Phys. Rev.* **2010**, *82*, 205111.
(45) Ziółkowski, M.; Jansík, B.; Kjærgaard, T.; Jørgensen, P. *J. Chem. Phys.* **2010**, *133*, 014107.
(46) Mata, R. A.; Stoll, H. *Chem. Phys. Lett.* **2008**, *465*, 136−141.
(47) Mata, R. A.; Stoll, H. *J. Chem. Phys.* **2011**, *134*, 034122.
(48) Kristensen, K.; Ziółkowski, M.; Jansík, B.; Kjærgaard, T.; Jørgensen, P. *J. Chem. Theory Comput.* **2011**, *7*, 1677−1694.
(49) Hoyvik, I.-M.; Kristensen, K.; Jansík, B.; Jørgensen, P. *J. Chem. Phys.* **2012**, *136*, 014105.
(50) Bates, D. M.; Smith, J. R.; Janowski, T.; Tschumper, G. S. *J. Chem. Phys.* **2011**, *135*, 044123.
(51) Gordon, M. S.; Fedorov, D. G.; Pruitt, S. R.; Slipchenko, L. V. *Chem. Rev.* **2012**, *112*, 632−672.
(52) Werner, H.-J.; Schütz, M. *J. Chem. Phys.* **2011**, *135*, 144116.
(53) Neese, F.; Hansen, A.; Liakos, D. G. *J. Chem. Phys.* **2009**, *131*, 064103.
(54) Liakos, D. G.; Hansen, A.; Neese, F. *J. Chem. Theory Comput.* **2011**, *7*, 76−87.
(55) Riplinger, C.; Neese, F. *J. Chem. Phys.* **2013**, *138*, 034106.
(56) Zhang, J.; Dolg, M. *J. Chem. Theory Comput.* **2013**, *9*, 2992−3003.
(57) Pruitt, S. R.; Addicoat, M. A.; Collins, M. A.; Gordon, M. S. *Phys. Chem. Chem. Phys.* **2012**, *14*, 7752−7764.
(58) Fedorov, D. G.; Nagata, T.; Kitaura, K. *Phys. Chem. Chem. Phys.* **2012**, *14*, 7562−7577.
(59) Mochizuki, Y.; Yamashita, K.; Nakano, T.; Okiyama, Y.; Fukuzawa, K.; Taguchi, N.; Tanaka, S. *Theor. Chem. Acc.* **2011**, *130*, 515−530.
(60) Dahlke, E. E.; Truhlar, D. G. *J. Chem. Theory Comput.* **2007**, *3*, 1342.
(61) Dahlke, E. E.; Truhlar, D. G. *J. Chem. Theory Comput.* **2007**, *3*, 46.
(62) Dahlke, E. E.; Leverentz, H. R.; Truhlar, D. G. *J. Chem. Theory Comput.* **2008**, *4*, 33.
(63) Qi, H. W.; Leverentz, H. R.; Truhlar, D. G. *J. Phys. Chem. A* **2013**, *117*, 4486−4499.
(64) Hughes, T. F.; Bartlett, R. J. *J. Chem. Phys.* **2008**, *129*, 054105.
(65) Yang, W. *Phys. Rev. Lett.* **1991**, *66*, 1438−1441.
(66) Kobayashi, M.; Nakai, H. *Phys. Chem. Chem. Phys.* **2012**, *14*, 7629−7639.
(67) Stoll, H. *Chem. Phys. Lett.* **1992**, *191*, 548−552.
(68) Nesbet, R. K. *Phys. Rev.* **1967**, *155*, 51−55.
(69) Doll, K.; Dolg, M.; Fulde, P.; Stoll, H. *Phys. Rev. B* **1995**, *52*, 4842−4848.
(70) Stoll, H.; Paulus, B.; Fulde, P. *J. Chem. Phys.* **2005**, *123*, 144108.
(71) Schmitt, I.; Fink, K.; Staemmler, V. *Phys. Chem. Chem. Phys.* **2009**, *11*, 11196−11206.
(72) Anacker, T.; Friedrich, J. *J. Comput. Chem.* **2014**, *35*, 634−643.
(73) Friedrich, J.; Yu, H.; Leverentz, H. R.; Bai, P.; Siepmann, J. I.; Truhlar, D. G. *J. Phys. Chem. Lett.* **2014**, *5*, 666−670.
(74) Zhang, J., Heinz, N., Dolg, M.**2014***537*700−7708.
(75) Li, S.; Shen, J.; Li, W.; Jiang, Y. *J. Chem. Phys.* **2006**, *125*, 074109.
(76) Li, W.; Guo, Y.; Li, S. *Phys. Chem. Chem. Phys.* **2012**, *14*, 7854−7862.
(77) Rolik, Z.; Kallay, M. *J. Chem. Phys.* **2012**, *135*, 104111.
(78) Rolik, Z.; Szegedy, L.; Ladjánszki, I.; Ladóczki, B.; Kállay, M. *J. Chem. Phys.* **2013**, *139*, 094105.
(79) Saebø, S.; Pulay, P. *J. Chem. Phys.* **1987**, *86*, 914−922.
(80) Werner, H.-J. *J. Chem. Phys.* **2008**, *129*, 101103.
(81) Adler, T. B.; Werner, H.-J. *J. Chem. Phys.* **2011**, *135*, 144117.
(82) Adler, T. B.; Werner, H.-J. *J. Chem. Phys.* **2009**, *130*, 241101.
(83) Venkatnathan, A.; Szilva, A. B.; Walter, D.; Gdanitz, R.; Carter, E. *J. Chem. Phys.* **2004**, *120*, 1693.
(84) Pisani, C.; Schütz, M.; Casassa, S.; Usvyat, D.; Maschio, L.; Lorenz, M.; Erba, A. *Phys. Chem. Chem. Phys.* **2012**, *14*, 7615−7628.
(85) Russ, N. J.; Crawford, T. *J. Chem. Phys.* **2004**, *121*, 691−696.
(86) Mata, R. A.; Werner, H.-J. *J. Chem. Phys.* **2006**, *125*, 184110.
(87) Friedrich, J.; Tew, D. P.; Klopper, W.; Dolg, M. *J. Chem. Phys.* **2010**, *132*, 164114.
(88) Vogiatzis, K. D.; Barnes, E.; Klopper, W. *Chem. Phys. Lett.* **2011**, *503*, 157−161.
(89) Vogiatzis, K. D.; Haunschild, R.; Klopper, W. *Theor. Chem. Acc.* **2014**, *133*, 1446.
(90) Friedrich, J.; Dolg, M. *J. Chem. Theory Comput.* **2009**, *5*, 287−294.
(91) Friedrich, J. *J. Chem. Theory Comput.* **2010**, *6*, 1834−1842.
(92) Friedrich, J.; Walczak, K. *J. Chem. Theory Comput.* **2013**, *9*, 408−417.
(93) Friedrich, J.; Hänchen, J. *J. Chem. Theory Comput.* **2013**, *9*, 5381−5394.

DOI: 10.1021/ct5011888
J. Chem. Theory Comput. XXXX, XXX, XXX−XXX

(94) Nyden, M. R.; Petersson, G. A. *J. Chem. Phys.* **1981**, *75*, 1843−1862.
(95) Friedrich, J.; Hanrath, M.; Dolg, M. *J. Phys. Chem. A* **2007**, *111*, 9830−9837.
(96) Friedrich, J.; Hanrath, M.; Dolg, M. *Chem. Phys.* **2007**, *338*, 33−43.
(97) Friedrich, J.; Hanrath, M.; Dolg, M. *Z. Phys. Chem.* **2010**, *224*, 513−525.
(98) Friedrich, J.; Dolg, M. *J. Chem. Phys.* **2008**, *129*, 244105.
(99) Friedrich, J.; Perlt, E.; Roatsch, M.; Spickermann, C.; Kirchner, B. *J. Chem. Theory Comput.* **2011**, *7*, 843−851.
(100) Spickermann, C.; Perlt, E.; Domaros, M.; Roatsch, M.; Friedrich, J.; Kirchner, B. *J. Chem. Theory Comput.* **2011**, *7*, 868−875.
(101) Anacker, T.; Friedrich, J. *Mol. Phys.* **2013**, *111*, 1161−1172.
(102) Bachorz, R. A.; Bischoff, F. A.; Glöss, A.; Hättig, C.; Höfener, S.; Klopper, W.; Tew, D. P. *J. Comput. Chem.* **2011**, *32*, 2492−2513.
(103) Köhn, A.; Tew, D. P. *J. Chem. Phys.* **2010**, *132*, 024101.
(104) Vogiatzis, K. D.; Klopper, W. *Mol. Phys.* **2013**, *111*, 2299−2305.
(105) Ahnen, S.; Hehn, A.-S.; Vogiatzis, K. D.; Trachsel, M. A.; Leutwyler, S.; Klopper, W. *Chem. Phys.* **2014**, *441*, 17−22.
(106) Mavrandonakis, A.; Vogiatzis, K. D.; Fink, K.; Heine, T.; Klopper, W. *Inorg. Chem.* **2014**, submitted.
(107) Ahlrichs, R.; Bär, M.; Häser, M.; Horn, H.; Kölmel, C. *Chem. Phys. Lett.* **1989**, *162*, 165−169.
(108) Schäfer, A.; Horn, H.; Ahlrichs, R. *J. Chem. Phys.* **1992**, *97*, 2571−2577.
(109) Weigend, F.; Häser, M.; Patzelt, H.; Ahlrichs, R. *Chem. Phys. Lett.* **1998**, *294*, 143−152.
(110) Ten-no, S. *Chem. Phys. Lett.* **2004**, *398*, 56−61.
(111) Tew, D. P.; Klopper, W. *J. Chem. Phys.* **2005**, *123*, 074101.
(112) Peterson, K. A.; Adler, T. B.; Werner, H.-J. *J. Chem. Phys.* **2008**, *128*, 84102−84114.
(113) Hill, J. G.; Mazumder, S.; Peterson, K. A. *J. Chem. Phys.* **2010**, *132*, 054108.
(114) Yousaf, K. E.; Peterson, K. A. *J. Chem. Phys.* **2008**, *129*, 184108−184115.
(115) Klopper, W.; Samson, C. C. M. *J. Chem. Phys.* **2002**, *116*, 6397.
(116) Ten-no, S. *J. Chem. Phys.* **2004**, *121*, 117−129.
(117) Becke, A. D. *Phys. Rev. A* **1988**, *38*, 3098−3100.
(118) Vosko, S. H.; Wilk, M.; Nusair, M. *Can. J. Phys.* **1980**, *58*, 1200.
(119) Perdew, J. P. *Phys. Rev. B* **1986**, *33*, 8822−8824.
(120) Treutler, O.; Ahlrichs, R. *J. Chem. Phys.* **1995**, *102*, 346−354.
(121) Eichkorn, K.; Weigend, F.; Treutler, O.; Ahlrichs, R. *Theor. Chem. Acc.* **1997**, *97*, 119−124.
(122) Eichkorn, K.; Treutler, O.; Öhm, H.; Häeser, M.; Ahlrichs, R. *Chem. Phys. Lett.* **1995**, *242*, 283.
(123) Deglmann, P.; May, K.; Furche, F.; Ahlrichs, R. *Chem. Phys. Lett.* **2004**, *384*, 103.
(124) Grimme, S.; Antony, J.; Ehrlich, S.; Krieg, H. *J. Chem. Phys.* **2010**, *132*, 154104.
(125) Li, W.; Piecuch, P.; Gour, J. R.; Li, S. *J. Chem. Phys.* **2009**, *131*, 114109.
(126) Yoo, S.; Apra, E.; Zeng, X. C.; Xantheas, S. S. *J. Phys. Chem. Lett.* **2010**, *1*, 3122−3127.
(127) Polenz, I.; Schmidt, F. G.; Friedrich, J.; Tchernook, I.; Spange, S. *Macromol. Chem. Phys.* **2013**, *214*, 1473−1483.
(128) Eddaoudi, M.; Kim, J.; Rosi, N.; Vodak, D.; Wachter, J.; O'Keeffe, M.; Yaghi, O. M. *Science* **2002**, *295*, 469−472.
(129) Rosi, N. L.; Eckert, J.; Eddaoudi, M.; Vodak, D. T.; Kim, J.; O'Keeffe, M.; Yaghi, O. M. *Science* **2003**, *300*, 1127−1129.
(130) Farha, O. K.; Hupp, J. T. *Acc. Chem. Res.* **2010**, *43*, 1166−1175.
(131) Lin, Y.; Yan, Q.; Kong, C.; Chen, L. *Sci. Rep.* **2013**, *3*, 1859.
(132) Banerjee, R.; Furukawa, H.; Britt, D.; Knobler, C.; O'Keeffe, M.; Yaghi, O. M. *J. Am. Chem. Soc.* **2009**, *131*, 3875−3877.
(133) Sun, D.; Ma, S.; Ke, Y.; Collins, D. J.; Zhou, H.-C. *J. Am. Chem. Soc.* **2006**, *128*, 3896−3897.
(134) Tonigold, M.; Lu, D. Y.; Mavrandonakis, A.; Puls, A.; Staudt, R.; Möllmer, J.; Sauer, J.; Volkmer, D. *Chem.—Eur. J.* **2011**, *17*, 8671−8695.
(135) Halder, G. J.; Kepert, C. J.; Moubaraki, B.; Murray, K. S.; Cashion, J. D. *Science* **2002**, *298*, 1762−1765.
(136) Liu, Y.; Eubank, J.-F.; Cairns, A.-J.; Eckert, J.; Kravtsov, V.-C.; Luebke, R.; Eddaoudi, M. *Angew. Chem., Int. Ed.* **2007**, *46*, 3278−3283.
(137) Mavrandonakis, A.; Klopper, W. *J. Phys. Chem. C* **2008**, *112*, 3152−3154.
(138) Doran, J. L.; Hon, B.; Leopold, K. R. *J. Mol. Struct.* **2012**, *1019*, 191−195.
(139) Farbos, B.; Tassaing, T. *Phys. Chem. Chem. Phys.* **2009**, *11*, 5052−5061.
(140) Morris, W.; He, N.; Ray, K. G.; Klonowski, P.; Furukawa, H.; Daniels, I. N.; Houndonougbo, Y. A.; Asta, M.; Yaghi, O. M.; Laird, B. B. *J. Phys. Chem. C* **2012**, *116*, 24084−24090.
(141) Babarao, R.; Dai, S.; Jiang, D. *Langmuir* **2011**, *27*, 3451−3460.
(142) Chen, L.; Cao, F.; Sun, H. *Int. J. Quantum Chem.* **2013**, *113*, 2261−2266.
(143) Dubbeldam, D.; Frost, H.; Walton, K. S.; Snurr, R. Q. *Fluid Phase Equilib.* **2007**, *261*, 152−161.

DOI: 10.1021/ct5011888
J. Chem. Theory Comput. XXXX, XXX, XXX−XXX